Orbital hybridization and spin polarization in the resonant 1*s* photoexcitations of α-Fe_2O_3

Pieter Glatzel,* Alessandro Mirone, Sigrid G. Eeckhout, and Marcin Sikora
European Synchrotron Radiation Facility, 6 rue Jules Horowitz, Boîte Postale 220, 38043 Grenoble, France

Gabriele Giuli
Dipartimento di Scienze della Terra and Unitá CNISM, Universitá di Camerino, Via Gentile III da Varano, 62032 Camerino, Italy
(Received 28 October 2007; revised manuscript received 8 January 2008; published 25 March 2008)

A spin-selective and polarization dependent study at the *K* absorption pre-edge in hematite (α-Fe_2O_3) was performed by means of 1*s*3*p* resonant x-ray emission spectroscopy on a single crystal. The experimental results can be modeled using a band structure approach [local density approximation (LDA + *U*)]. The spin-selective spectra in connection with the calculations firmly establish metal-oxygen and metal-metal orbital hybridizations. A phase shift in the polarization dependent absorption cross section is observed between the first two absorption features showing directionality in the orbital hybridization.

DOI: 10.1103/PhysRevB.77.115133 PACS number(s): 71.70.Ch, 61.05.cj, 71.70.Gm, 87.64.kd

I. INTRODUCTION

The properties of 3*d* transition metal compounds are being intensely studied but many aspects concerning the electronic and magnetic structure remain elusive despite considerable experimental and theoretical advances. Element-selective techniques such as inner-shell spectroscopies have been a widely used approach over the past decades. The 3*d* shell can be directly probed by measuring the metal 2*p*-3*d* absorption spectrum.[1] *L*-edge absorption spectroscopy is an established tool to study electronic configurations also because the strong spin-orbit interaction in the 2*p* shell renders the *L*-edge sensitive to magnetic properties.[2,3]

In many cases it is, however, experimentally more favorable to use a hard x-ray probe at the metal *K* edge. This gives more freedom with respect to sample environment for studies in, e.g., extreme conditions or to monitor chemical reactions. The unpaired spin in the 1*s* core hole of the excited state interacts only weakly with the valence electrons and the absence of an orbital moment in the core hole excludes spin-orbit coupling in the core hole as well as a core hole induced anisotropy in contrast to *L*-edge excited states. This should considerably facilitate theoretical calculations. Still, the assignment of spectral features in the *K* absorption pre-edges of transition metals is discussed controversially. The weak transitions at the onset of the *K* absorption main edge can often be calculated using different and sometimes mutually exclusive theoretical models.[4–10]

Spectral intensity in the pre-edge arises from dipole and quadrupole transition matrix elements. Electron-electron interactions in the valence shell can give a rich multiplet structure[7,11] and cause multielectron excitations.[12] Crystal field effects and orbital hybridization furthermore need to be taken into account in a theoretical analysis. A particularly interesting aspect is orbital hybridization between metal atoms that can give rise to spectral intensity in the pre-edge range and results in an excited state with an electron that is delocalized over the neighboring metal atoms.[4,13–17]

There is thus a wealth of possible mechanisms that can be invoked to explain the pre-edge spectral features. It is therefore desirable to apply a more stringent test of the theory since not all theoretical models put forward to date can be correct. This can be achieved by accessing additional experimental parameters that are related to the pre-edge as it is done in resonant x-ray emission and polarization dependent studies.

The excited states that give rise to the 3*d* transition metal *K* absorption pre-edge decay with a fluorescence yield of about 80%.[18] The emitted X-rays can be analyzed with an instrumental energy bandwidth similar to that of the incident beam using a wavelength dispersive spectrometer [resonant x-ray emission spectroscopy[19] (RXES)].[20] By scanning incident and emitted energy, a two-dimensional intensity distribution is obtained.[12,21] The RXES plane contains considerable more information about the electronic structure and the excitation process than just the absorption pre-edge. One application of this technique is spin-selective 1*s*3*p* RXES spectroscopy where the final states contain a hole in the 3*p* shell.

Figure 1 shows the principle for hematite (α-Fe_2O_3). Three absorption features (intermediate states A, B, and C) have been identified in the pre-edge region (*vide infra*). The final states are reached via a 3*p* to 1*s* transition. The 3*p* core hole in the final state strongly interacts with the unpaired

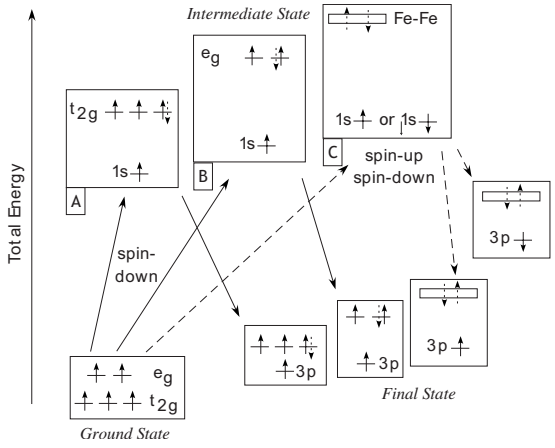

FIG. 1. Energy level diagram for 1*s*3*p* RXES in hematite. Orbital notations are used in SO_3 symmetry for core levels and O_h symmetry for Fe 3*d* levels. The peak assignments A, B, and C refer to Figs. 3 and 4.

spin in the metal 3*d* shell via the (3*p*,3*d*) exchange interaction, which leads to a line splitting of approximately 15 eV for Fe. The non-resonant $K\beta$ lines in Fe compounds have been studied in detail.[20,22–24]

The $K\beta_{1,3}$ and $K\beta'$ fluorescence lines correspond to final states with the unpaired spin in the 3*p* shell either parallel or antiparallel to the unpaired spin in the 3*d* shell. This alignment is conserved upon the $K\beta$ 3*p* to 1*s* transition following the selection rule $\Delta s=0$ if spin-orbit interactions can be neglected. The final states thus select the spin orientation of the 1*s* hole and, as a direct consequence, the spin orientation of the photoexcited electron.[25,26] Within this interpretation, the $K\beta$ spectra are not sensitive to the magnetic ordering of a system. They merely reflect the local spin state as confirmed by 3*p* photoemission experiments on free metal atoms.[28] The spin-selective absorption, however, may show a dependence on the magnetic ordering.

A detailed theoretical study of the spin selectivity has been presented by Wang *et al.*[27] Non-diagonal Coulomb matrix elements as well as spin-orbit interaction can mix electronic states with different spin in the valence shell and the spin-selectivity is only approximately valid. For the present work, it is important that the 3*p* spin-down ($K\beta'$) final state (cf. Fig. 1) provides very high spin-selectivity.[27] A 1*s*3*p* RXES investigation on Fe_2O_3 has been performed by Yamaoka *et al.*[29] We extend their study by discussing Fe-Fe orbital hybridization supported by local density approximation (LDA+*U*) calculations.

Another experimental parameter that can be varied in a XAS experiment on single crystals using synchrotron radiation is the orientation of the crystal axes with respect to the polarization direction of the incident x-ray beam with linear polarization. The intensity variation of the absorption cross section with the angular orientation depends on the nature of the transition (dipole or quadrupole) as well as the electronic configuration in the final state.[30] Polarization dependent studies combined with RXES (and resonant elastic scattering) have been shown to be a powerful tool to establish the nature of electronic transitions and to identify spectral features.[14,31–34]

The symmetry of the unit cell in α-Fe_2O_3 is D_{3d}.[35] The magnetic order exhibits antiparallel alignment of the Fe spins along the *c*-axis and an in-plane parallel alignment. Iron is six coordinated in α-Fe_2O_3 in a distorted octahedra (Fig. 2) and the local symmetry of one FeO_6 cluster is C_3 neglecting the electron spins. Due to the absence of parity as a good quantum number, the unoccupied density of states (DOS) with respect to the Fe center does not separate into distinct gerade and ungerade states. The DOS with *p* symmetry (ungerade) with respect to the Fe center thus occurs at the same energies as the *d*-DOS (gerade) just above the Fermi level. As a result, dipole transitions are expected to strongly contribute to the *K* absorption pre-edge spectral intensity.

The origin of the three pre-edge absorption features in hematite has not yet been resolved. Two features can be readily accounted for as transitions to crystal field split orbitals. The third peak C (cf. Figs. 1 and 3) has been tentatively assigned to unoccupied states that are formed by Fe-Fe orbital hybridization.[16,36] This is a central point in the discussion of pre-edges since electron sharing between metal centers in non-metallic systems can be an important aspect to explain electronic and magnetic properties. This paper therefore presents a detailed experimental study of the hematite pre-edge supported by LDA+*U* calculations.

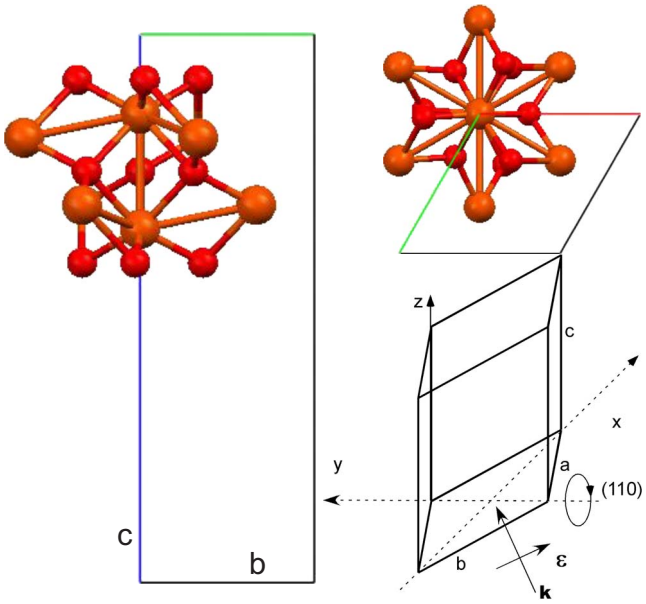

FIG. 2. (Color online) Structure and unit cell of hematite; the geometry for the polarization dependent studies is shown.

II. EXPERIMENT

The experiment was performed at beamline ID26 of the European Synchrotron Radiation Facility (ESRF). The incident energy was selected by means of a pair of cooled Si crystals in (220) reflection with an energy bandwidth of 0.5 eV at 7.1 keV. The incident flux on the sample was 5×10^{12} photons/s using the fundamental undulator peak. The beam size on the sample was 0.35 mm horizontal by 1.0 mm

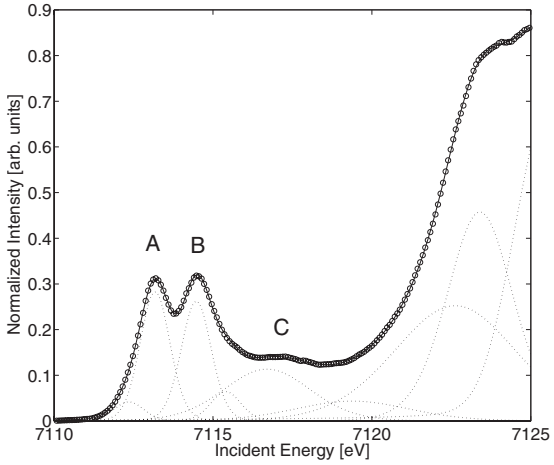

FIG. 3. PearsonVII functions (dotted lines; solid line: sum) fitted to the *K* pre-edge spectral features for the spin-up spectrum with experimental rotation angle at 60° (circles).

vertical. Higher harmonics were suppressed by two Si mirrors operating in total reflection. Total fluorescence yield absorption spectra were recorded using a Si photodiode.

The resonantly scattered x-rays were analyzed using the (531) reflection of a spherically bent Si wafer and an avalanche photodiode arranged with the sample in a horizontal, point-to-point (scanning) Rowland geometry ($R=1$ m). The combined instrumental energy bandwidth was 1.3 eV and the scattering angle was 90°. The hematite single crystal is a natural sample collected on Elba Island. It was cut and polished along the (110) plane.

The geometry for the polarization dependent studies is shown in Fig. 2. We show in all figures the experimental rotation angle where 0° corresponds to the polarization $\boldsymbol{\varepsilon}$ in the (a,b) plane and 90° experimental angle implies 45° between $\boldsymbol{\varepsilon}$ and the crystal c axis.

All spectra—total fluorescence yield as well as spin selective—are normalized to the K edge jump. The pre-edge spectral features were fitted together with the rising edge using a PearsonVII parametrization of Voigt profiles (Fig. 3). Two peaks were used to fit each feature A and B. This is motivated by considering a symmetry that is lower than O_h around the Fe atoms with additional orbital splitting. Fitting of the remaining spectral intensity is arbitrary. The broad feature C introduces a large uncertainty for the fitting of feature B. Furthermore, the spectra were not corrected for self-absorption effects, i.e., the pre-edge intensities relative to the edge jump are not correct. The angles that determine the self-absorption were not changed during the experiment, i.e., the spectral distortions due to self-absorption do not change. Therefore, the conclusions drawn in this work are not influenced by self-absorption effects.

III. CALCULATIONS

The absorption coefficient can be related to the density of empty states projected on symmetries with orbital angular momentum $l=1$ (p-DOS, dipole transitions) or $l=2$ (d-DOS, quadrupole transitions) with respect to the absorbing atom. It is necessary to consider the core hole in the theoretical model. Band-structure calculations were performed using the WIEN2K code with local density approximation and local correlations $[\mathrm{LDA}+U^{(d+p)}]$ including exchange interactions (J). We use $U-J=6$ eV both for iron and oxygen.[37,38] In order to determine the effect of the core hole, we removed one $1s$ electron on one of the four Fe atoms in the unit cell (the photoexcited or absorber Fe*). We then ran a self-consistent field (SCF) calculation with a frozen absorber $3d$ shell. The WIEN2K code uses a linearized augmented plane wave basis and the freezing is achieved by choosing a high value for the energy around which the d atomic orbitals are linearized.[39] For sufficiently high linearization energies, the occupied valence orbitals have a vanishing d-partial density of state (d-DOS) at the frozen site. This density of states is reintroduced in the calculation adding a $3d$ entry to the file from which WIEN2K reads the list of core orbitals. The occupancy of the $3d$ shell and its spin polarization are first fixed by hand and the SCF calculation is performed. In the WIEN2K code, the core orbitals are also calculated self-consistently. Once the calculation has converged, the potential is stored, and another unfrozen non-SCF calculation is run. We recover, in particular, the partial density of states for the $3d$ band at the previously frozen site.

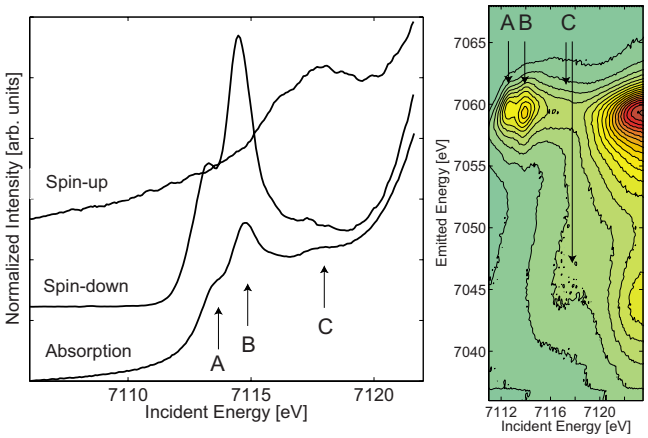

FIG. 4. (Color online) Left: total and spin-selective absorption in Fe_2O_3 for $\boldsymbol{\varepsilon}\perp\mathbf{c}$. Right: $1s3p$ RXES plane for polycrystalline Fe_2O_3. The spin-up and spin-down excitations occur around 7045 and 7059 eV emitted energies, respectively.

The $3d$ occupation value for the frozen system is chosen to match the resulting d-DOS to the one for an unfrozen SCF calculation. The match was done for a fractional hole and then extrapolated to one charge unit hole. It is not possible to use a non-frozen SCF calculation for one full charge hole because the $3d$ occupancy versus hole charge has a discontinuity between 0 and 1 which corresponds to an electronic transition and not to electronic relaxation.

IV. RESULTS AND DISCUSSION

A. Spin-dependent absorption

Figure 4 shows the absorption pre-edge decomposed into spin components using $1s3p$ RXES spectroscopy as well as the full $1s3p$ RXES plane as a contour plot. The three absorption pre-edge features A, B, and C are separated in the spin-selective spectra where peaks A and B are absent in the spin-up direction and C shows intensity for both spin directions of the photoexcited electron. The RXES plane conveys the same information and confirms the presence of three absorption and four emission features. Structure C is broad and not as distinct as features A and B which can indicate a strongly delocalized electron distribution.

For simplicity, we assign the first two peaks A and B to t_{2g} and e_g orbitals, respectively, neglecting for the moment the additional, smaller splitting of the orbitals due to the reduction of the symmetry from O_h to C_3. Fe^{3+} in Fe_2O_3 has a high-spin $3d^5$ configuration and we expect that only the spin-down intermediate states show intensity for the t_{2g} and e_g lines (cf. Fig. 1). However, the argument is only valid if spin-orbit interactions can be neglected such that spin remains a good quantum number and electronic states with different spin states do not mix. The pre-edge excited state of an isolated Fe^{3+} ion is $1s3d^6$ with a $^5D_4$ configuration for the

$3d$ shell in the LS coupling scheme,[40] i.e., a non-zero orbital angular momentum and thus non-negligible spin-orbit interaction. The $1s3p$ RXES experimental results on hematite, however, show pure spin selectivity within the experimental accuracy. The orbital angular momentum in the pre-edge excited states up to 7116 eV excitation energy is therefore negligible due to the reduced symmetry of the Fe ion in the solid ("quenching" of the orbital moment).[41] Spin mixing could occur in systems with higher symmetry and thus non-zero orbital angular momentum such that $1s3p$ RXES spectroscopy in, for example, octahedral Mn(II) complexes (also high-spin $3d^5$) might exhibit a reduced spin sensitivity.

The third peak C at 7118 eV incident energy in Fig. 4 shows intensity for both spin directions indicating excitations into a delocalized band that provides unoccupied spin-up and spin-down densities. It is possible to identify localized and delocalized states by analyzing the dispersion of the peak intensity (Raman shift). This approach is based on theoretical work as reviewed by Kotani and Shin[42] as well as Gel'mukhanov and Ågren.[43] An illustrative discussion of the Raman shift in the RXES plane is presented in Ref. 12. However, the analysis can lead to ambiguous results since the dispersion can be strongly influenced by the instrumental energy broadening. Also, if the core hole lifetime broadening is larger than the splitting of energy levels, a band cannot necessarily be distinguished from discrete, i.e., possibly localized, energy levels (as pointed out by Gel'mukhanov and Ågren[43]). Furthermore, a sharp feature that exhibits a Raman shift, i.e., a resonant excitation into a final state with discrete energy, can still arise from a delocalized orbital, e.g., in molecular complexes. Finally, the analysis of the peak dispersion requires unambiguous identification of the peak position for all incident energies. This is not always possible (cf. Fig. 4, RXES plane). We thus refrain from this approach and interpret the spectra theoretically based on an LDA+U approach.

The DOS on the photoexcited Fe as obtained from the LDA+U calculations is shown in Fig. 5 separated into spin-up and spin-down contributions. The Fermi energy is at 0 eV. In the d-DOS, the fist two peaks in the unoccupied states show the statistical intensity ratio for t_{2g} and e_g assignments. The p-DOS, however, shows the experimentally observed intensity ratio. Orbital hybridization changes the spectral intensity ratio of $I(t_{2g}):I(e_g)=3:2$ according to the statistical weight for ionic orbitals. Thus, spectral intensity cannot arise from quadrupole transition matrix elements only. The p-DOS furthermore shows structures for both spin directions at about 5 eV above the Fermi level. This corresponds to the experimental observation for the third absorption prepeak structure C. The calculations thus confirm the dominant dipole character in all pre-edge features of hematite. The first peak in the DOS above 0 eV shows a double structure which reflects the distortion and deviation from O_h symmetry. The splitting is not observed in the experiment due to insufficient spectral resolution even though we considered the splitting in the pre-edge fitting procedure (*vide supra*).

The d-DOS for the equatorial and axial Fe (Fig. 5) confirm that the structures around 5 eV in the calculated p-DOS for the photoexcited Fe (Fe*) arise from the d-DOS on the neighboring Fe atoms. The spin-down DOS can be assigned to the coplanar, spin-aligned Fe, and the spin-up DOS origins from the out-of-plane Fe atoms along the crystal c axis with antiparallel spin orientation.

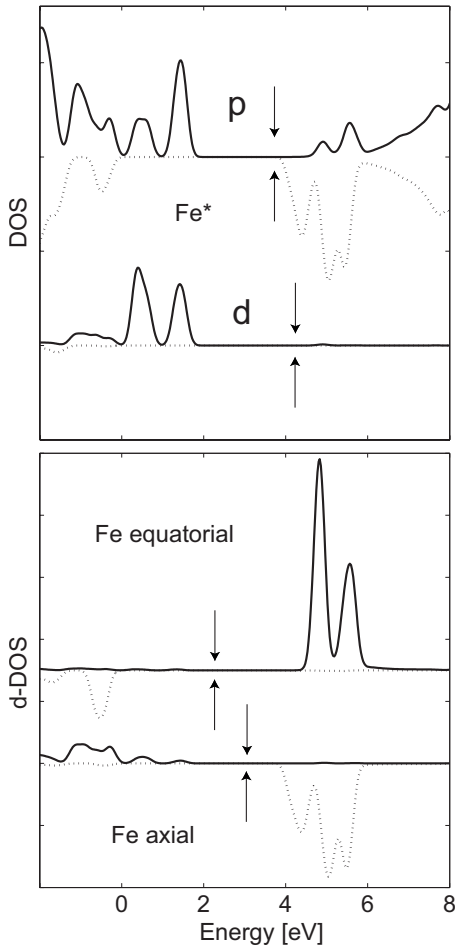

FIG. 5. Top: density of states (DOS) decomposed into p and d symmetries with respect to the excited Fe (Fe*) atom. The p-DOS is scaled by a factor of 500. Bottom: d-DOS with respect to the neighboring (equatorial and axial) Fe atoms. For each symmetry, the spin-up (dotted) and spin-down (solid) densities are shown.

The orbitals that give rise to the pre-edge are thus orbitals containing p contribution with respect to the central, photoexcited Fe atom. Peaks A and B are assigned to orbitals that are localized on the excited Fe atom with mainly $3d$ character. They obtain some p character from hybridization with O ligand $2p$ orbitals. The p character gives rise to most of the spectral intensity. We find that the DOS at higher energies shows contributions from neighboring Fe $3d$ orbitals that have p character with respect to the photoexcited Fe. Thus, the transitions forming peak C arise from excitations between two Fe atoms (metal-metal excitation).

B. Polarization-dependent absorption

The validity of the theoretical model can be further tested by angular dependent studies on a single crystal. The intensity variation is governed by the crystal symmetry and not

the local symmetry around the metal atom.[30] Dräger *et al.* performed angular dependent studies in hematite and found only weak quadrupole contributions in agreement with our findings.[44]

The crystal symmetry in hematite is rhombohedral and the angular dependence of the absorption cross section has the form $(3\cos^2\theta-1)$ for dipole transitions with θ being the angle between the crystal c axis and the polarization vector.[30] Figure 6 shows the spin-down absorption edges with varying angles between $\boldsymbol{\varepsilon}$ and the crystal c axis. The calculated p-DOS for the two experimental polarizations, i.e., the spin-down p_c-DOS corresponding to $\boldsymbol{\varepsilon}\|\mathbf{c}$ and p_c+p_a (or p_b) DOS for angle$(\boldsymbol{\varepsilon},\mathbf{c})=45°$ reproduces the experimentally observed change in intensity for peaks A and B. However, the calculated DOS does not yield the correct ratio between peaks A and B for angle$(\boldsymbol{\varepsilon},\mathbf{c})=45°$ pointing to shortcomings of our theoretical model that are most likely to be found in the approximative treatment of electron-electron interactions and the core hole effect. A fit assuming a dipolar angular dependence matches the experimental data (Fig. 6, inset). The error bar mainly arises from the ambiguity of assigning spectral intensity to either feature A or B in the fitting procedure. The experimental error is too large for a quantitative analysis of the amount of quadrupole contribution. For that purpose, the measurements performed by Dräger *et al.* are more suitable.[44]

The experimentally observed inverse change in intensity for peaks A and B is nicely reproduced in the calculations. This corresponds to a phase shift of 90° in the θ angular dependence between the two spectral features as would be expected for quadrupole excitations into t_{2g} and e_g orbitals.[30] The symmetries in the dipole transition matrix elements for $1s$ absorption in D_{3d} symmetry are, assuming A_{1g} symmetry for the $1s$ shell, $\langle A_{1g}|A_{2u}|A_{2u}\rangle$ for $\boldsymbol{\varepsilon}\|\mathbf{c}$ and $\langle A_{1g}|E_u|E_u\rangle$ for $\boldsymbol{\varepsilon}\perp\mathbf{c}$. The angular dependence (cf. Fig. 6) thus shows that peak A contains more A_{2u} contribution, while peak B has stronger E_u contribution. We now consider one approximately octahedral $[FeO_6]$ cluster where the xy, yz, and zx orbitals are between and the x^2-y^2 and $3z^2-r^2$ orbitals along the Fe-O bonds. The xy, yz, and zx orbitals are located at lower energies than the x^2-y^2 and $3z^2-r^2$ orbitals according to crystal field theory. The Fe xy, yz, and zx orbitals thus hybridize with the ligand orbitals to form electronic states with mainly A_{2u} symmetry (peak A) with the p-DOS oriented along the crystal c axis, while the x^2-y^2 and $3z^2-r^2$ orbitals form states with E_u symmetry (peak B) with the p-DOS perpendicular to the c axis. With respect to the magnetic ordering in hematite where alternate Fe layers are polarized in opposite direction along the c axis, this means that the Fe xy, yz, and zx orbitals strongly hybridize in the direction of antiferromagnetic ordering. Note that we use the local symmetry C_3 of a FeO_6 cluster to explain p-d hybridization and the crystal symmetry D_{3d} to interpret the polarization dependent results.

We do not observe any spin or angular dependence for the third structure C within the experimental error while this is predicted by the calculations. The spectral intensity between the first two peaks and the main edge is not fully accounted for in the theoretical DOS. Multielectron transitions (such as shake transitions) upon core hole creation are not included in the theoretical model. These are expected to occur shifted toward higher energies relative to peaks A and B since additional energy is required to excite the second electron. Thus, the unaccounted additional spectral features probably mask

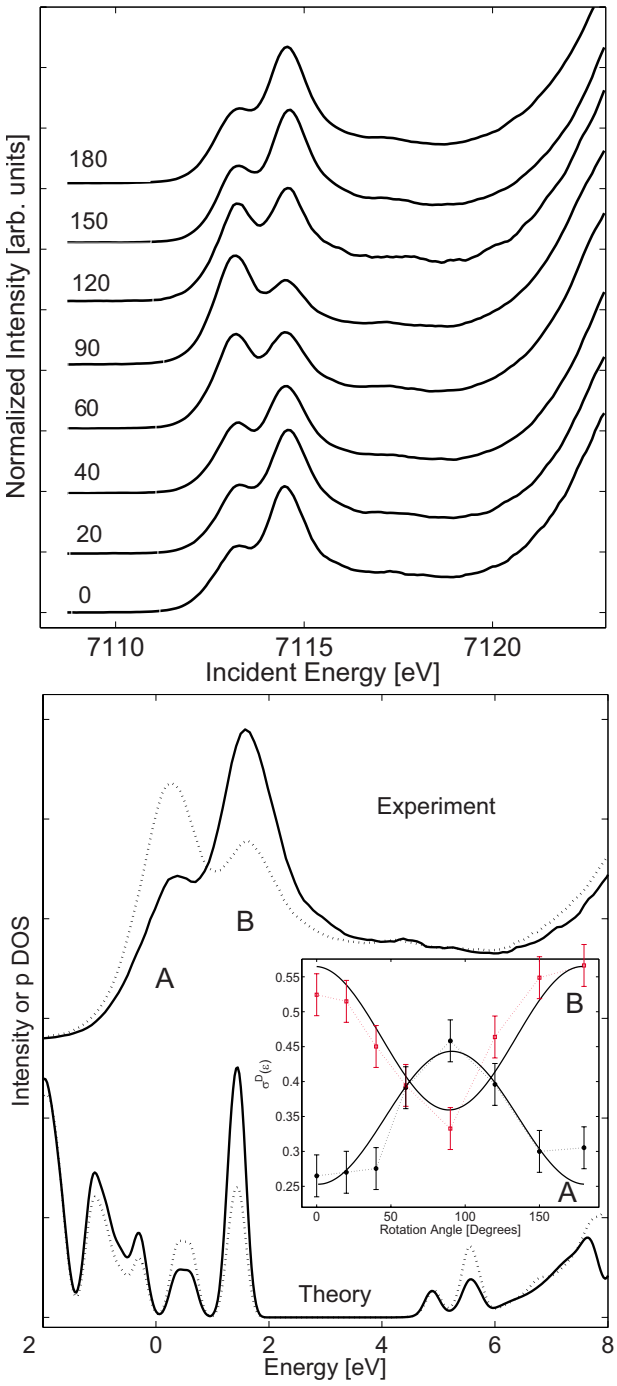

FIG. 6. (Color online) Top panel: angular dependent pre-edge spectra in hematite for spin-down absorption. The experimental rotation angle is given (cf. Fig. 2). Bottom panel: (top) pre-edge absorption with $\boldsymbol{\varepsilon}\perp\mathbf{c}$ (solid) and angle$(\boldsymbol{\varepsilon},\mathbf{c})=45°$ (dashed) and (bottom) calculated p-DOS for the two cases. The experimental energy axis was shifted to match the theoretical values. The inset shows the area under peaks A and B versus the experimental rotation angle together with the theoretical dipole dependence.

the angular effect predicted by our LDA+U calculations for feature C of the hematite pre-edge.

A study of the linear dichroism by Prince *et al.* at the oxygen K edge[45] reports a change of the crystal field splitting from 1.3 with $\boldsymbol{\varepsilon}$ parallel to 1.5 eV with $\boldsymbol{\varepsilon}$ perpendicular to the crystal c axis. While the splitting between the maxima of peaks A and B of 1.35 eV in our measurements nicely agrees with the results by Prince *et al.*, we do not observe any polarization dependent change in the peak splitting.

Furthermore, we do not observe any temperature dependence in the pre-edge spectral shape (spectra not shown) in contrast to the L edge study by Kuiper *et al.*[3] While small changes in the electron orbital configuration when going below the Morin temperature accompany the reorientation of the electron spins,[46] we do not expect to be sensitive to such changes at the K edge. Due to the absence of core hole spin-orbit interaction as well as final state multiplet splittings, the K pre-edge of hematite is not directly sensitive to magnetic effects as opposed to the L edge. We note, however, that van Aken and Lauterbach did observe a temperature induced change in the O K edge of hematite by electron energy loss spectroscopy measurements.[47] Like the Fe K pre-edge, the O K edge is also not directly sensitive to magnetic effects and the changes should therefore reflect the change in electron orbital configuration. We do not have an explanation why the changes are visible at the O K edge and not at the Fe K pre-edge other than smaller instrumental broadening at the O K edge.

V. CONCLUSIONS

We give a comprehensive account for the K absorption pre-edge of Fe in hematite by taking advantage of the information contained in spin-selective and angular dependent absorption spectroscopy in connection with LDA+U calculations. The use of a variety of experimental parameters firmly establishes the theoretical interpretation. The considerable influence of orbital hybridization of metal-ligand and metal-metal type on the spectral shape points to the importance of electron delocalization for the understanding of electronic and magnetic properties.

We note that a Fe(III) system with a dominantly $3d^5$ configuration is a favorable case with respect to electronic structure calculations due to the half-filled $3d$ shell. We think that the procedure presented here is a promising approach for the investigation of electronic structure in $3d$ transition metals. However, an extension to more complex systems such as Mn in manganites requires more sophisticated theoretical models that properly take electron-electron interactions and the core hole effect into account. To our knowledge, such a theory is not available to date.

ACKNOWLEDGMENT

We are grateful to Sergio Di Matteo for valuable discussions. We thank Christophe Lapras and the ESRF support groups.

*glatzel@esrf.fr

[1] F. M. F. de Groot, J. Electron Spectrosc. Relat. Phenom. **676**, 529 (1994).
[2] B. T. Thole, P. Carra, F. Sette, and G. van der Laan, Phys. Rev. Lett. **68**, 1943 (1992).
[3] P. Kuiper, B. G. Searle, P. Rudolf, L. H. Tjeng, and C. T. Chen, Phys. Rev. Lett. **70**, 1549 (1993).
[4] F. Farges, Phys. Rev. B **71**, 155109 (2005).
[5] P. Glatzel, U. Bergmann, J. Yano, H. Visser, J. H. Robblee, W. W. Gu, F. M. F. de Groot, G. Christou, V. L. Pecoraro, S. P. Cramer, and V. K. Yachandra, J. Am. Chem. Soc. **126**, 9946 (2005).
[6] Y. Joly, D. Cabaret, H. Renevier, and C. R. Natoli, Phys. Rev. Lett. **82**, 2398 (1999).
[7] T. E. Westre, P. Kennepohl, J. G. DeWitt, B. Hedman, K. O. Hodgson, and E. I. Solomon, J. Am. Chem. Soc. **119**, 6297 (1997).
[8] Z. Y. Wu, D. C. Xian, T. D. Hu, Y. N. Xie, Y. Tao, C. R. Natoli, E. Paris, and A. Marcelli, Phys. Rev. B **70**, 033104 (2004).
[9] R. V. Vedrinskii, V. L. Kraizman, A. A. Novakovich, P. V. Demekhin, and S. V. Urazhdin, J. Phys.: Condens. Matter **10**, 9561 (1998).
[10] S. D. George, P. Brant, and E. I. Solomon, J. Am. Chem. Soc. **127**, 667 (2005).
[11] L. Hozoi, A. H. de Vries, and R. Broer, Phys. Rev. B **64**, 165104 (2001).
[12] P. Glatzel and U. Bergmann, Coord. Chem. Rev. **249**, 65 (2005).
[13] Q. Qian, T. A. Tyson, C. C. Kao, M. Croft, and A. Y. Ignatov, Appl. Phys. Lett. **80**, 3141 (2002).
[14] A. Shukla, M. Calandra, M. Taguchi, A. Kotani, G. Vanko, and S. W. Cheong, Phys. Rev. Lett. **96**, 077006 (2006).
[15] Z. Y. Wu, D. C. Xian, C. R. Natoli, A. Marcelli, E. Paris, and A. Mottana, Appl. Phys. Lett. **79**, 1918 (2001).
[16] F. M. F. de Groot, P. Glatzel, U. Bergmann, P. A. van Aken, R. A. Barrea, S. Klemme, M. Havecker, A. Knop-Gericke, W. M. Heijboer, and B. M. Weckhuysen, J. Phys. Chem. B **109**, 20751 (2005).
[17] M. Wilke, F. Farges, P. E. Petit, G. E. Brown, and F. Martin, Am. Mineral. **86**, 714 (2001).
[18] M. O. Krause, J. Phys. Chem. Ref. Data **8**, 307 (1979).
[19] In order to distinguish the present technique from spectroscopies where the emitted energy differs from the energy of a fluorescence line by considerably more than the magnitude of electron-electron or spin-orbit interactions, here we use the term RXES as opposed to resonant inelastic x-ray scattering (RIXS).
[20] See, e.g., A. Meisel, G. Leonhardt, and R. Szargan, *X-Ray Spectra and Chemical Binding* (Springer-Verlag, New York, 1989). "Wavelength dispersive" describes the fact that Bragg's law is used as opposed to energy dispersive solid state detectors.
[21] J. P. Rueff, L. Journel, P. E. Petit, and F. Farges, Phys. Rev. B **69**, 235107 (2004).
[22] S. D. Gamblin and D. S. Urch, J. Electron Spectrosc. Relat. Phenom. **113**, 179 (2001).
[23] P. Glatzel, U. Bergmann, F. M. F. de Groot, and S. P. Cramer,

Phys. Rev. B **64**, 045109 (2001).
[24] G. Vanko, T. Neisius, G. Molnar, F. Renz, S. Karpati, A. Shukla, and F. M. F. de Groot, J. Phys. Chem. B **110**, 11647 (2006).
[25] K. Hämäläinen, C. C. Kao, J. B. Hastings, D. P. Siddons, L. E. Berman, V. Stojanoff, and S. P. Cramer, Phys. Rev. B **46**, 14274 (1992).
[26] G. Peng, A. X. Wang, C. R. Randall, J. A. Moore, and S. P. Cramer, Appl. Phys. Lett. **65**, 2527 (1994).
[27] X. Wang, F. M. F. deGroot, and S. P. Cramer, Phys. Rev. B **56**, 4553 (1997).
[28] A. von dem Borne, R. L. Johnson, B. Sonntag, M. Talkenberg, A. Verweyen, P. Wernet, J. Schulz, K. Tiedtke, C. Gerth, B. Obst, P. Zimmermann, and J. E. Hansen, Phys. Rev. A **62**, 052703 (2000).
[29] H. Yamaoka, M. Oura, M. Taguchi, T. Morikawa, K. Takahiro, A. Terai, K. Kawatsura, A. M. Vlaicu, Y. Ito, and T. Mukoyama, J. Phys. Soc. Jpn. **73**, 3182 (2004).
[30] C. Brouder, J. Phys.: Condens. Matter **2**, 701 (1990).
[31] M. Taguchi, J. C. Parlebas, T. Uozumi, A. Kotani, and C. C. Kao, Phys. Rev. B **61**, 2553 (2000).
[32] H. Shoji, M. Taguchi, E. Hirai, T. Iwazumi, A. Kotani, S. Nanao, and Y. Isozumi, J. Phys. Soc. Jpn. **72**, 1560 (2003).
[33] G. Subias, J. Garcia, M. G. Proietti, J. Blasco, H. Renevier, J. L. Hodeau, and M. C. Sanchez, Phys. Rev. B **70**, 155105 (2004).
[34] D. Z. Cruz, M. Abbate, H. Tolentino, P. J. Schiling, E. Morikawa, A. Fujimori, and J. Akimitsu, Phys. Rev. B **59**, 12450 (1999).
[35] R. L. Blake, R. E. Hessevick, T. Zoltai, and L. W. Finger, Am. Mineral. **51**, 123 (1966).
[36] W. A. Caliebe, C. C. Kao, J. B. Hastings, M. Taguchi, A. Kotani, T. Uozumi, and F. M. F. de Groot, Phys. Rev. B **58**, 13452 (1998).
[37] I. A. Nekrasov, M. A. Korotin, and V. I. Anisimov, arXiv:cond-mat/0009107v1 (unpublished) (2000).
[38] G. K. H. Madsen and P. Novak, Europhys. Lett. **69**, 777 (2005).
[39] G. K. H. Madsen and P. Novak, *Calculating the Effective U in APW Methods: NiO* (WIEN2k, Vienna, 2007), http://www.wien2k.at/reg_user/textbooks/Constraint_U.pdf
[40] R. D. Cowan, *The Theory of Atomic Structure and Spectra* (University of California Press, Berkeley, 1981).
[41] J. S. Griffith, *The Theory of Transition-Metal Ions* (Cambridge University Press, Cambridge, England, 1964).
[42] A. Kotani and S. Shin, Rev. Mod. Phys. **73**, 203 (2001).
[43] F. Gel'mukhanov and H. Ågren, Phys. Rep. **312**, 91 (1999).
[44] G. Dräger, R. Frahm, G. Materlik, and O. Brümmer, Phys. Status Solidi B **146**, 287 (1988).
[45] K. C. Prince, F. Bondino, M. Zangrando, M. Zacchigna, K. Kuepper, M. Neumann, and F. Parmigiani, J. Electron Spectrosc. Relat. Phenom. **144**, 719 (2005).
[46] W. C. Mackrodt, F. Jollet, and M. Gautier-Soyer, Philos. Mag. B **79**, 25 (1999).
[47] P. A. van Aken and S. Lauterbach, Phys. Chem. Miner. **30**, 469 (2003).